

# Validating an analytical method to predict flexural behavior of RC T-beams retrofitted with bonded steel wire ropes in the negative moment region

Cite as: AIP Conference Proceedings 2482, 030001 (2023); <https://doi.org/10.1063/5.0113554>  
Published Online: 21 February 2023

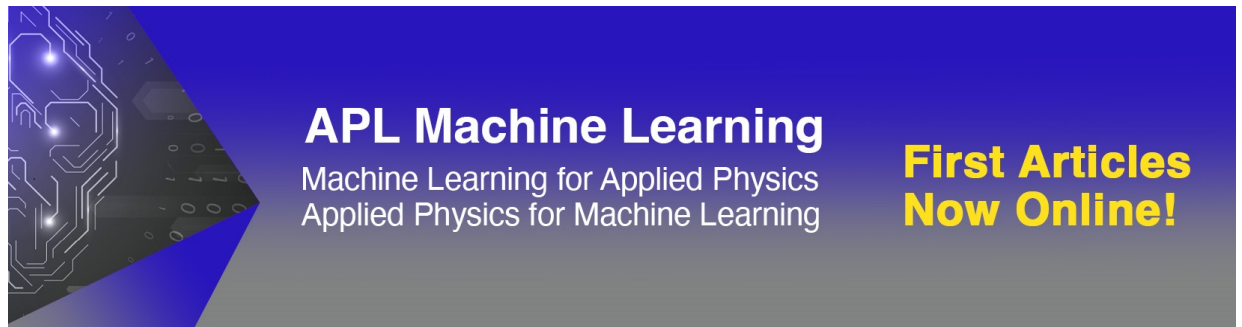
Yanuar Haryanto, Fu-Pei Hsiao, Hsuan-Teh Hu, et al.



[View Online](#)



[Export Citation](#)



**APL Machine Learning**  
Machine Learning for Applied Physics  
Applied Physics for Machine Learning

**First Articles  
Now Online!**

# Validating an Analytical Method to Predict Flexural Behavior of RC T-Beams Retrofitted with Bonded Steel Wire Ropes in the Negative Moment Region

Yanuar Haryanto<sup>1, 2, a)</sup>, Fu-Pei Hsiao<sup>1, 3, b)</sup>, Hsuan-Teh Hu<sup>1, 4, c)</sup>, Ay Lie Han<sup>5, d)</sup>, Banu Ardi Hidayat<sup>1, 5, e)</sup>, Laurencius Nugroho<sup>1, f)</sup>

<sup>1</sup>*Department of Civil Engineering, College of Engineering, National Cheng Kung University, No. 1 University Road, Tainan, 701, Taiwan (R.O.C).*

<sup>2</sup>*Department of Civil Engineering, Faculty of Engineering, Jenderal Soedirman University, Jln. Mayjen. Sungkono KM 5, Blater, Purbalingga, 53371, Indonesia.*

<sup>3</sup>*National Center for Research on Earthquake Engineering, 200 Sec. 3 Xinhai Road, Taipei, 10668, Taiwan (R.O.C).*

<sup>4</sup>*Department of Civil and Disaster Prevention Engineering, College of Engineering and Science, National United University, No. 2 Lien Da, Nan Shih Li, Miaoli, 36063, Taiwan (R.O.C).*

<sup>5</sup>*Department of Civil Engineering, Faculty of Engineering, Diponegoro University, Jln. Prof. Soedarto, Tembalang, Semarang, 50375, Indonesia.*

a) Corresponding author: yanuar.haryanto@unsoed.ac.id

b) fphsiao@ncree.narl.org.tw

c) hthu@mail.ncku.edu.tw

d) hanaylie@live.undip.ac.id

e) banuardihidayat@lecturer.undip.ac.id

f) laurenciusnugroho@gmail.com

**Abstract.** In this day and age, a rewarding and new structural strengthening technique for civil structures is steel wire rope (SWR) strengthening. The ideal technique for structural analysis is the finite element method. Nonetheless, it could be an expensive and a challenging task to develop a model through the finite element method for a simple problem, for instance, cross section analysis of reinforced concrete (RC) structures. Therefore, in order to predict the flexural behavior of T-section RC beams, strengthened in the negative moment region with bonded steel wire ropes, researchers performed an analytical validation through a program based on the modified compression field theory (MCFT), namely Response-2000. They chose experimental data from the test conducted on three T-section RC beams in 2012. Subsequently, the collected results were compared with calculations from the fiber-elements method, constructed in excel spread sheets. Reasonably precise calculations of load-deflection responses, up to the peak load, were offered by the developed analytical model, however, the ductility of the beams was underestimated. The validated model was then utilized to study the impact of SWR diameter on the behavior of strengthened beams. This analytical investigation reveals the effectiveness of SWR bonded systems as an alternative strengthening technique, with the aim of enhancing the flexural capacity of RC beams.

## INTRODUCTION

Civil engineering structures, such as buildings, face constant external environmental effects, natural disasters (e.g. earthquakes [1-6]), changes in their function [7] and other, unforeseen, overloading factors [8]. Consequently, the aging and damage to the structures during their serviceable life, usually undermines their loading capacities. Good flexibility properties, low weight, high strength and ease of installation are the benefits of steel wire rope (SWR), which has become a revolutionary structural strengthening technique for civil structures [9]. Researchers

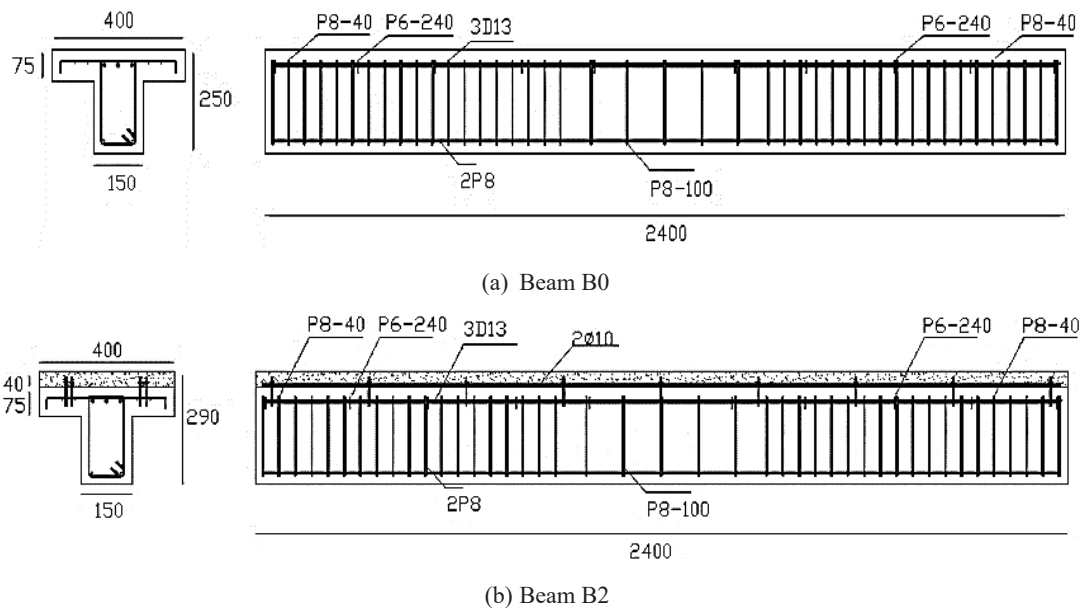
have universally explored the behavior of reinforced concrete (RC) structures strengthened with steel wire rope [10-16]. To date, the finite element method is the leading technique available for structural analysis. Nevertheless, for a simple problem, such as the cross sectional analysis of RC structures, it would be an expensive and complex task to perform modeling with the finite element method [17]. Bentz [18] developed “Response-2000” (hereafter denoted as R2K) as one of the sectional analysis programs through which the full load-deformation response of a reinforced concrete cross-section can be computed, depending on the shear, moment and axial load, on the basis of modified compression field theory (MCFT) [19]. R2K is a reliable, quick analysis tool with an excellent ability to predict experimental behavior [20-24].

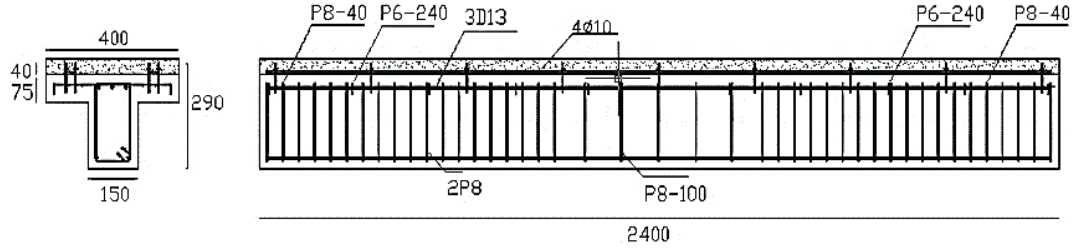
A technique, namely fiber-elements, has also been developed for modeling the non-linear post-yield response behavior of composite structures to extreme loading, such as RC elements in a cracked state [25-27]. A comparative analysis of the fiber-elements of T-beams was carried out by Galuh [28]. A study of RC T-beams, flexurally-strengthened with steel wire rope using R2K and fiber-elements, was performed by Atmajayanti [29], who revealed that the ratios of the flexural capacity on account of the analysis using R2K and fiber-elements, were 1.01 and 1.04, respectively, when compared to the outcomes of the control beam; 0.84 and 0.87 were recorded as the ratios of the strengthened beam. Lam et al. [30] performed a study on force-deformation behavior, modeling cracked reinforced concrete using fiber-elements and the R2K program. Furthermore, for all the cross-sections under consideration, researchers have gauged a similar moment of resistance. In this paper, an analytical method based on the modified compression field theory (MCFT) built in R2K is used to predict the flexural behavior of T-section RC beams, strengthened in the negative moment region with bonded steel wire ropes. Subsequently, the collected results were compared with calculations from the fiber-elements method, constructed in excel spread sheets. The validated model was then utilized to study the impact of SWR diameter on the behavior of strengthened beams.

## ANALYTICAL MODEL DEVELOPMENT

### Geometric Features

A holistic, elevation view of the beam specimens and their cross-sectional details are shown in Figure 1. In addition, Table 1 is indicative of the full description and designation of the tested specimens for analytical modeling. Along with a control beam specimen (B0), two 10 mm diameter steel wire ropes were employed to strengthen one of the beams (B2), while four 10 mm diameter steel wire ropes were used to support the other one (B4). The steel wire rope was bonded with 40 mm thick mortar throughout the total length of the beam specimens, along their longitudinal axis.





(c) Beam B4

FIGURE 1. Geometric details of modeled T-section RC beam specimens (mm)

TABLE 1. Description of RC T-beams for analysis

Specimens	L (mm)	bf (mm)	tf (mm)	bw (mm)	tw (mm)	Longitudinal reinforcement		Stirrup		Steel wire rope
						Tensile	Compression	Edge of span	Center of span	
B0	2400	400	75	150	175	3D13	2P8	P8-40	P8-100	–
B2	2400	400	115	150	175	3D13	2P8	P8-40	P8-100	2φ10
B4	2400	400	115	150	175	3D13	2P8	P8-40	P8-100	4φ10

## Constitutive Laws

### Concrete

For concrete and mortar, the average compressive strength ( $f'_c$ ) obtained was recorded as 32.39 MPa and 49.85 MPa, respectively. Concerning R2K, the developed analytical models considered the nonlinear properties of concrete under compression, through defining the strain-stress relations. As per equations (1)-(3), this model was developed by Popoviccs [31] and Porasz [32], who adjusted it to some extent. Moreover, as per equations (4)-(6), the calculations by the fiber-elements method were determined through the Hognestad model [33].

$$f_c = - \left( \frac{\varepsilon_c}{\varepsilon_{co}} \right) f'_c \frac{n}{n-1 + \varepsilon_c / \varepsilon_{co} n^k} \quad (1)$$

$$n = 0.8 + \frac{f'_c}{17} \quad (2)$$

$$k = \begin{cases} 1.0 & \text{if } \varepsilon_c / \varepsilon_{co} < 1.0 \\ 0.67 + \frac{f'_c}{62} & \text{if } \varepsilon_c / \varepsilon_{co} > 1.0 \end{cases} \quad (3)$$

$$f_c = f'_c \left[ \frac{2\varepsilon_c}{\varepsilon_{co}} - \left( \frac{\varepsilon_c}{\varepsilon_{co}} \right)^2 \right] \quad \text{where } 0 \leq \varepsilon_c \leq \varepsilon_{co} \quad (4)$$

$$f_c = f'_c - \left[ \frac{0.5f'_c}{\varepsilon_c - \varepsilon_{co}} \right] (\varepsilon_c - \varepsilon_{co}) \quad \text{where } \varepsilon_c > \varepsilon_{co} \quad (5)$$

$$\varepsilon_{co} = \frac{2f'_c}{E_c} \quad (6)$$

where:

$f_c$  = concrete compressive stress in MPa, corresponding to the specified strain value  $\varepsilon_c$

$f'_c$  = concrete compressive strength in MPa

$E_c$  = concrete modulus of elasticity in MPa

$\varepsilon_{co}$  = strain at peak compressive strength

$n$  = curve fit parameter

$k$  = factor of loss in post-peak ductility for high strength concrete

As per equation (7), Bentz [20] proposed a model for the nonlinear material attributes of concrete under tension ( $f_t$ ) that were employed in R2K. Moreover, as per equation (8), the computations with the fiber-elements method were carried out by following the William and Warnke model [35] adopted in SNI 2847: 2013 [35].

$$f_t = 0.45 f'_c{}^{0.4} \quad (7)$$

$$f_t = 0.62 \sqrt{f'_c} \quad (8)$$

### *Ductile Steel Reinforcement*

The mechanical properties of the utilized reinforcing bars were investigated through uniaxial coupon tensile tests. As far as 8 mm diameter plain bars are concerned, the factors, such as average elastic modulus, tensile strength and yield strength were 201.642 GPa, 525.330 MPa and 373.850 MPa, respectively. In the case of deformed 13 mm diameter bars, the corresponding average elastic modulus, tensile strength and yield strength obtained were 197.664 GPa, 742.520 MPa and 479.710 MPa.

An initial linear-elastic response, a yield plateau, and either a linear or nonlinear strain-hardening phase until rupture, are the three basic parts that constitute most of the reinforcement stress-strain response. As discussed below, for the hysteretic response, the back-bone curve of the Seckin [36] or Menegotto-Pinto [37] models are described by this monotonic stress-strain curve. In addition, equation (9) determines the reinforcement stress  $f_s$  in tension and compression.

$$f_s = \begin{cases} E_s \varepsilon_s & \text{for } \varepsilon_s < \varepsilon_y \\ f_y & \text{for } \varepsilon_y < \varepsilon_s \leq \varepsilon_{sh} \\ f_u + f_y - f_u \left( \frac{\varepsilon_u - \varepsilon_s}{\varepsilon_u - \varepsilon_{sh}} \right) & \text{for } \varepsilon_{sh} < \varepsilon_s \leq \varepsilon_u \\ 0 & \text{for } \varepsilon_u < \varepsilon_s \end{cases} \quad (9)$$

where  $\varepsilon_s$  is the reinforcement strain ( $\varepsilon_s = |\varepsilon_s|$ ),  $\varepsilon_y$  is the yield strain,  $\varepsilon_{sh}$  is the strain at the onset of the strain hardening,  $\varepsilon_u$  is the ultimate strain,  $E_s$  is the elastic modulus,  $f_y$  is the yield strength,  $f_u$  is the ultimate strength, and  $P$  is the strain-hardening parameter. There are two options for the strain-hardening phases after the yield plateau. These are linear strain-hardening (trilinear,  $P = 1$ ) and nonlinear strain-hardening ( $P = 4$ ), as assigned to the developed analytical models in R2K. For computations in the fiber-elements method, elastic-plastic or bilinear stress-strain curves were generated from the trilinear option. The strain hardening modulus  $E_{sh}$  was defined by equation (10).

$$E_{sh} = \left( \frac{f_u - f_y}{\varepsilon_u - \varepsilon_{sh}} \right) \quad (10)$$

### *Steel Wire Rope*

For 10 mm diameter steel wire ropes, the tensile strength and average elastic modulus obtained were 743.73 MPa and 32.568 GPa, respectively. The steel wire rope stress-strain response used in R2K and the fiber-elements method

was reliant on the behavior of cold-worked steel reinforcement. A distinct yield plateau is not exhibited by this behavior, however, the presentation entailed an initial linear-elastic branch and a transition curve to a second hardening linear branch. As per equations (11)-(14), the Ramsberg-Osgood formulation [38] was employed to determine the steel wire rope stress  $f_s$  in tension.

$$f_c = E_s \varepsilon_s \left\{ A + \frac{1-A}{\left[1 + B \varepsilon_s^c\right]^{1/C}} \right\} \leq f_u \quad (11)$$

$$A = \frac{E_{sh}}{E_s} \quad (12)$$

$$B = \frac{E_s (1-A)}{f_s^*} \quad (13)$$

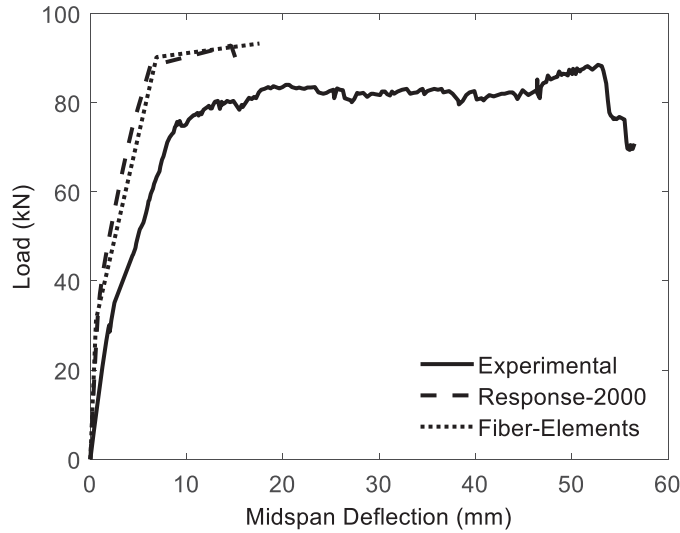
$$C = \text{transition coefficient} \quad (14)$$

where  $E_s$  is the initial elastic modulus,  $\varepsilon_s$  is the reinforcement strain,  $f_u$  is the ultimate strength and  $f_s^*$  is the value at which the stress axis is intercepted at zero strain by the second linear branch. A representative transition coefficient value  $C$  of 6 was obtained for stress-relieved steel, 10 for low-relaxation steel.

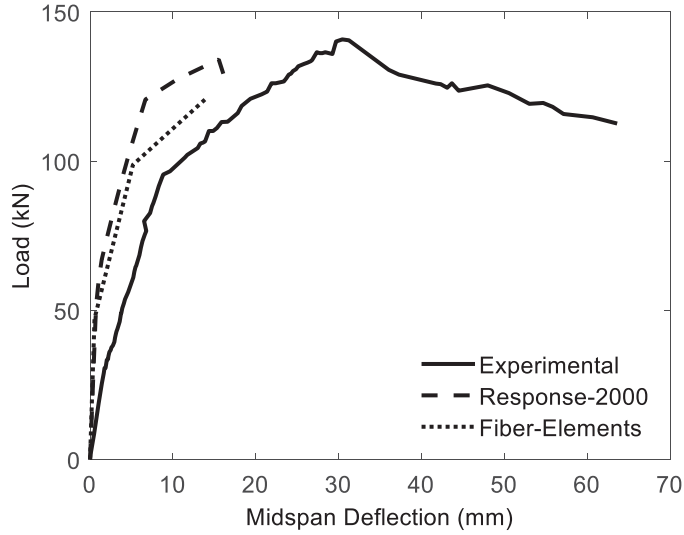
## RESULTS AND DISCUSSION

### Model Validation

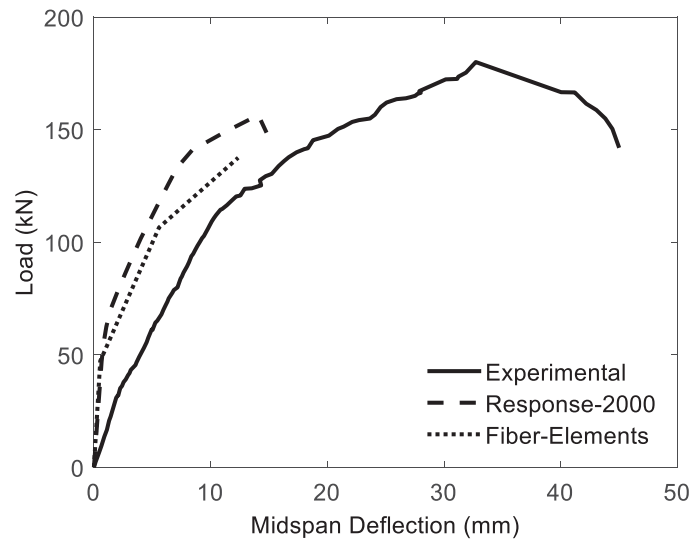
Researchers modeled and analyzed the three tested specimens to authenticate and ensure the precision of the developed analytical models. Afterwards, a comparison was made between the predicted data from the R2K program and the experimental data obtained and the fiber-elements method (henceforth called Analytical-1 and Analytical-2). At all stages of loading, the experimental and predicted load versus mid-span deflection results are displayed in Figure 2. Moreover, the values of predicted and experimentally calculated ultimate attained load ( $P_u$ ) are compared in Table 2. Likewise, for the ultimate load values, the ratio of the experimental over the predicted values ( $P_{u,Exp}/P_{u,An.1}$ ) and ( $P_{u,Exp}/P_{u,An.2}$ ) is also given in Table 2.



(a) Beam B0



(b) Beam B2



(c) Beam B4

**FIGURE 2.** Load-deflection curve comparisons between experimental and predicted values

**TABLE 2.** Results verification between experimental and analytical models

Beam ID	$P_u$ (kN)			Ratio	
	Experimental	Analytical-1	Analytical-2	$P_{u,Exp}/P_{u,An-1}$	$P_{u,Exp}/P_{u,An-2}$
B0	88.50	92.82	93.27	0.95	0.94
B2	140.80	134.07	120.63	1.05	1.15
B4	180.00	156.45	137.49	1.15	1.30

As far as the analytical predictions shown in Figure 2 are concerned, it is quite clear that the experimental responses are closely replicated by the predicted responses. An initial linear-elastic response is anticipated for each beam, where a transitional nonlinear response and a final, somewhat linear, response tend to follow it until the peak load is reached. This agreement is remarkable because it takes into account the complication of the actual response originating from the propagation of pre-existing cracks and the formation of concrete cracks. In this manner, the overall stiffness of the beam decreases. Nonetheless, an undesirable response was found near the peak. In particular,

the ductility of the beams is likely to be under-estimated by the analytical predictions. Since for Analytical-1 and Analytical-2, the Normalized Mean Square Error (NMSE) is 0.011 and 0.045, and if the prediction of load capacity (as required from the design point of view) is taken into account, this state of affairs is still tolerable. To study the impact of SWR diameter and the performance of RC beams strengthened in the negative moment region with bonded technique, the design oriented parametric study could then use the developed analytical model.

### Parametric Study on the Effect of SWR Diameter

Researchers have established four models with respect to Analytical-1, with the aim of examining the behavior of the beam upon adjustment of the SWR diameter. They have modeled one of the beams as a controlled un-strengthened specimen and the two bonded SWR were employed to strengthen the remaining three models with diameters of 8, 10 and 12 mm, respectively. The concrete and mortar compressive strength of 35 and 45 MPa was applied to the analyzed models. Figure 3 represents the predicted load versus mid-span displacement response curves for each model. Moreover, Table 3 offers the designation for each analyzed model. This table also encapsulates and compares the predicted ultimate attained load ( $P_u$ ) along with its corresponding mid-span deflection ( $\delta_u$ ).

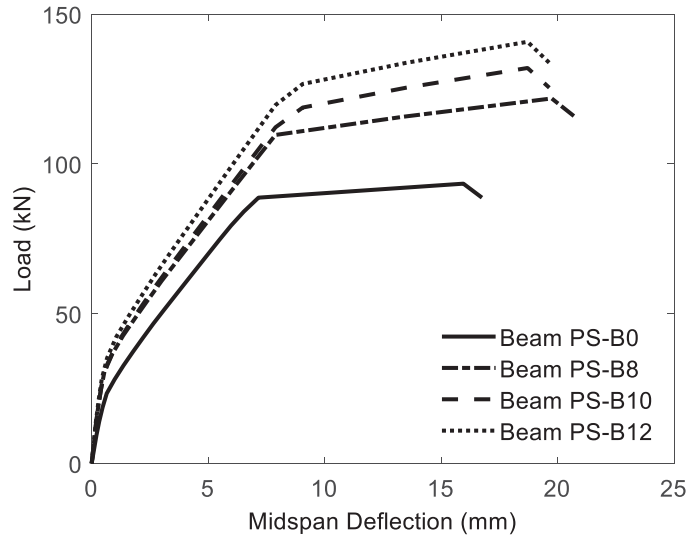


FIGURE 3. Load versus deflection curves for specimens of different SWR diameters

TABLE 3. Effect of varying SWR diameter

Beam ID	SWR diameter (mm)	$P_u$ (kN)	% $P_u$ increase over PS-B0	$\delta_u$ (mm)
PS-B0	-	93.39	-	15.95
PS-B8	8	121.84	30.46	19.75
PS-B10	10	132.01	41.35	18.71
PS-B12	12	140.75	50.71	17.99

Table 3 and Figure 3 clearly reveal that the beams having bonded SWR in the negative moment region (fulfilling expectations) and a higher load-carrying capacity (flexural strength) was accomplished compared to the control beam (PS-B0). The load-carrying capacity ( $P_u$ ) of beam PS-B8 (8 mm diameter SWR) is higher than the control specimen (PS-B0) by 30.46%. Moreover, Table 3 also depicts that the increase in  $P_u$  for beams PS-B10 (10 mm diameter SWR) and PS-B12 (12 mm diameter SWR) was 41.35% and 50.71%, respectively. Hence, it can be inferred that the increase in the size (diameter) of SWR and the percentage increase in the beam's load-carrying capacity are harmonious with each other. Since the diameter of SWR becomes augmented, it results in an increase in the moment arm of SWR tensile force. Therefore, the SWR-bonded strengthening technique yielded an overall efficiency enhancement. Remarkably, Figure 3 and Table 3 are indicative of the fact that, for all beam specimens, the mid-span deflection ( $\delta_u$ ) linked with  $P_u$  is comparable. Consequently, while preserving a sufficient level of



ductility in the strengthened beam specimens, an increase in the strength factor has been observed. This particular approach is useful as a different strengthening technique, to an extent, where there is an increase in the strength of T-section RC beams under negative moment loads.

## CONCLUSIONS

To analyze the flexural behavior of T-section RC beams strengthened in the negative moment region with bonded SWR, the outcomes of developed analytical models were presented in this study. The behavior and response of three beam specimens, with their peers from experimental tests, were compared in order to verify the models. Subsequently, to explore the impact of SWR diameter on the flexural performance of T-section RC beams, strengthened in the negative moment region with bonded SWR, a design-oriented parametric study then utilized the developed and validated models. This study has generated the following observations and conclusions:

- The flexural behavior of the tested T-section RC beam specimens, in the presence and absence of bonded SWR in the negative moment region, was reasonably simulated by the analytical models.
- The beams that were strengthened in the negative moment region with bonded SWR, exhibited an increase in beam load carrying capacity.
- The increase in the size (diameter) of SWR corresponds to the percentage increase in a beam's load-carrying capacity.
- As far as the negative moment region is concerned, the SWR bonded technique is beneficial in bringing improvements in the flexural capacity of T-section RC beams and this technique is seen as a substitute strengthening technique.

## ACKNOWLEDGMENTS

The authors would like to appreciate the Research and Public Services Institution (LPPM) of Jenderal Soedirman University, Indonesia, for providing the funding for the research.

## REFERENCES

1. Y. Haryanto, G. H. Sudibyo and F. C. A Effendi, *Procedia Eng.* **171**, 233 (2017).
2. Y. Haryanto, B. S. Gan, N. G. Wariyatno and E. W. Indriyati, *APRN J. Eng. Appl. Sci.* **12**, 4858 (2017).
3. Y. Haryanto, B. S. Gan, N. G. Wariyatno and E. W. Indriyati, *MATEC Web Conf.* **192**, (2018).
4. A. Widyaningrum, Y. Haryanto and N. I. S. Hermanto, *MATEC Web Conf.* **195**, (2018).
5. Y. Haryanto, H.-T. Hu, A. L. Han, B. A. Hidayat and E. W. Indriyati, *Aceh Int. J. Sci. Technol.* **8**, 1 (2019).
6. A. Widyaningrum, Y. Haryanto, G. H. Sudibyo and N. I. S. Hermanto, *J. Phys. Conf. Ser.* **1367**, (2019).
7. Y. Haryanto, B. S. Gan, A. Widyaningrum, A. Maryoto, *J. Teknol. (Sci Eng)* **79**, 233 (2017).
8. B. A. Hidayat, H.-T. Hu, A. L. Han, Y. Haryanto, A. Widyaningrum and G. Pamudji, *IOP Conf. Ser. Mater. Sci. Eng.* **615**, (2019).
9. X. Li, G. Wu, M. S. Popal and J. Jiang, *Constr. Build. Mater.* **188**, 456 (2018).
10. Y. Haryanto, I. Satyarno and D. Sulistyono, *Civ. Eng. For.* **21**, 1163 (2021).
11. Y. Haryanto, B. S. Gan and A. Maryoto, *Int. J. Technol.* **8**, 134 (2017).
12. Y. Haryanto, H.-T. Hu, A. L. Han, A. T. Atmajayanti, D. L. C. Galuh and B. A. Hidayat, *J. Teknol. (Sci Eng)* **81**, 143 (2019).
13. S. Y. Kim, K. H. Yang, H. Y. Byun and A. F. Ashour, *Eng. Struct.* **29**, 2711 (2007).
14. Y. Wei and Y. F. Wu, *Constr. Build. Mater.* **54**, 443 (2014).
15. Y. Haryanto, B. S. Gan, A. Widyaningrum, N. G. Wariyatno and A. Fadli, *J. Teknol. (Sci Eng)* **80**, 145 (2018).
16. Y. Haryanto, A. L. Han, H.-T. Hu, F.-P. Hsiao, B. A. Hidayat and A. Widyaningrum, *J. Chin. Inst. Eng.* **44**, 193 (2021).
17. R. Thamrin, *MATEC Web Conf.* **103**, (2017).
18. E. C. Bentz, "Sectional analysis of reinforced concrete members," Ph.D. thesis, University of Toronto, (2000).
19. F. J. Vecchio and M. P. Collins, *ACI J.* **83**, 219 (1986).
20. I. M. Metwally, *HBRC J.* **8** 9 (2012).
21. B. Suryanto, R. Morgan and A. L. Han, *Civ. Eng. Dim.* **8**, 16 (2016).

22. Z. Huang, Y. Tu, S. Meng, N. Bagge, J. Nilimaa and T. Blanksvärd, 2019 *Eng. Struct.* **197**, (2019).
23. Y. Haryanto, H.-T. Hu, A. L. Han, F.-P. Hsiao, C.-J. Teng, B. A. Hidayat and N. G. Wariyatno, *J. Chin. Inst. Eng.* **44**, (2021).
24. Y. Haryanto, H.-T. Hu, A. L. Han, F.-P. Hsiao, N. G. Wariyatno and B. A. Hidayat, *J. Eng. Sci. Technol.* **16**, (2021).
25. E. Spacone, F. C. Filippou and F. F. Taucer, *Earthq. Eng. Struct. Dyn.* **25**, 711 (1996).
26. E. Spacone, F. C. Filippou and F. F. Taucer, *Earthq. Eng. Struct. Dyn.* **25**, 727 (1996).
27. G. Monti and E. Spacone, *J. Struct. Eng. ASCE* **126**, 654 (2000)
28. D. L. C. Galuh, *IOP Conf. Ser.: Mater. Sci. Eng.* **316**, (2018).
29. A. T. Atmajayanti, *Din. Rek.* **9**, 34 (2013).
30. N. Lam , J. Wilson and E. Lumantarna, *Comput. Concr.* **8**, 43 (2011).
31. S. Popovics, *Cem. Concr. Res.* **3**, 483 (1973)
32. A. Porasz, “An investigation of the stress-strain characteristics of high strength concrete in shear,” Ph.D. thesis, University of Toronto, (1989).
33. E. Hognestad, N. W. Hanson and D. McHenry, *ACI J. Proc.* **52**, 475 (1955)
34. K. J. Willam and E. D. Warnke “Constitutive model for the triaxial behavior of concrete,” in Proceedings International Association for Bridge and Structural engineering (Bergamo: ISMES), (1975).
35. The National Standardization Agency of Indonesia, “SNI 2847:2013 Persyaratan beton struktural untuk bangunan Gedung,” (in Indonesian), (2013).
36. M. Seckin, “Hysteretic behaviour of cast-in-place exterior beam-column sub-assemblies,” Ph.D. thesis, University of Toronto, 1981.
37. M. Menegotto and P. E. Pinto, “Method of analysis for cyclically loaded reinforced concrete plane frames including changes in geometry and non-elastic behavior of elements under combined normal force and bending,” in ABSE Symposium of Resistance and Ultimate Deformability of Structures Acted on by Well-Defined Repeated Loads, (1973).
38. W. Ramberg and W. R. Osgood, “Description of stress-strain curves by three parameters,” Technical Note No. 902, National Advisory Committee for Aeronautics, (1943).